International Journal of Engineering Science and Applied Mathematics
Volume.14, Number 5; May-2022;
ISSN: 2836-9521| Impact Factor: 6.64
https://zapjournals.com/Journals/index.php/ijesam
Published By: Zendo Academic Publishing

MICROPOLAR FLUIDS PROPERTIES AND APPLICATIONS IN ENGINEERING AND SCIENCE

[1]Prathap Kumar, [2]Jawali Channabasappa Umavathi and [3]Appasaheb Sharanappa Dhone

Article Info

Keywords: micropolar fluids, non-Newtonian fluids, rheological models, couple stress sustenance, thermal energy, heat transfer, engineering, science.

Abstract

This paper presents an analysis of micropolar fluid past a wedge, considering the effects of viscous dissipation and heat absorption for flow systems doped with gyrotactic microorganisms. The transport model developed using nonlinear PDEs was transformed into a set of equivalent ODEs through suitable transformation equations. The shooting technique in micropolar fluid, in conjunction with the Runge-Kutta-Fehlberg integration scheme in microorganisms, was used to solve the obtained set of equations numerically. The effects of key factors on non-dimensional momentum profiles, temperature, and motile bioconvective Lewis microorganism density were estimated for the impact of pressure gradient parameter, Eckert number, material parameter, heat sink, and bioconvection Lewis number. The numerical data obtained was graphically presented, and the consequences of the major factors were thoroughly described in both the cases of Blasius and stagnation flow. Micropolar fluid is a type of fluid that displays microscopic impacts due to the phenomenon of fluid particle micromotion. The effectiveness of liquid crystals, lubricants, animal blood flowing through rigid cells, and other substances can be discussed using micropolar fluids. The unique feature of this fluid class is couple stress sustenance. This study is important for understanding the behaviour of micropolar fluids and can be applied in various fields, such as lubricants, cooling of metal plates in a bath tub, animal's blood, and physiological fluids, among other things. The numerical data obtained in this study provides new insights into the behaviour of micropolar fluids and can serve as a basis for further research in this field. Overall, this study provides valuable insights into the properties and applications of micropolar fluids in engineering and science.

[1] Department of Mathematics, Gulbarga University, Karnataka, India
[2] Department of Mathematics, Gulbarga University, Karnataka, India
[3] Department of Mathematics, Gulbarga University, Karnataka, India

1. INTRODUCTION

The viscosity law of Newton does not apply to non-Newtonian fluids. Because of industrial and engineering goals, the importance of non-Newtonian fluids has garnered a lot of attention in current years. Chemical reactions and lubricants, bioengineering materials, material fabrication, polymer mixes, and other applications necessitate the use of such fluids. Molten polymers, paints, scrub, blood, unguent, maquillage, and foods such as ketchup, cheese, honey, soups, taffy etc. are examples of non-Newtonian fluids, as are natural resources like petroleum, lava, and some kinds of dispersions. Food digesting, antibiotic dispensing, and biomedical sectors such as toxin elimination and cancer therapy may all have important responsibilities to consider. Because of the inclusion of rheological influences in their constituent regulating equations, non-Newtonian liquids and their dynamic properties have a lot of complications. Over the past 20 years, researchers' interest in the thermo-physical characteristics of these fluids has increased [1, 2]. In several disciplines of chemical and material processing engineering, non-Newtonian transport phenomenon occurs. Compared to the Newtonian (Navier-Stokes (N-S)) model, shear-stress-strain correlations in such fluids deviate greatly. In almost all non Newtonian models, the momentum conservation equations are altered in some way. Power-law, thixo-tropic, and visco-elastic fluids are among them [3]. However, microstructural features of many critical liquids, such as polymer suspensions, physiological fluids, contaminated lubricants, and so on, are impossible to simulate using such rheological models. Micropolar liquids are the name given to these types of liquids [4].

Micropolar fluid is a type of fluid that displays microscopic impacts due to the phenomenon of fluid particle micromotion. This fluid is made up of stiff macromolecules that move independently and maintain stress and body moment through spin inertia. The effectiveness of liquid crystals, lubricants, animal blood flowing through rigid cells, and other substances can be discussed using micropolar fluids [5]. These fluids are composed of randomly arranged particles dispersed in a sticky medium that can rotate and alter the flow's hydrodynamics, making them nonNewtonian fluids [6]. A unique feature of this fluid class is couple stress sustenance. Eringen [7] proposed the micropolar material model for microstructural fluids to overcome these challenges. Two new velocity variables are introduced in the micropolar fluid theories that were not included in the N-S model. These microrotational parameters reflect the spin and microinertia tensors that describe the distributions of atoms and molecules inside minute fluid particles. Following that, a number of researchers looked at the micropolar liquid from various angles [8-14]. It is used to investigate the behaviour of novel lubricants, liquid crystal solidification, and extraction of polymer fluid, cooling of metal plates in a bath tub, animal’s blood, and physiological fluids, among other things [15]. Eringen [16] went on to expand on the micropolar fluid idea and coined the term "thermomicropolar fluids". The implication of chemical reactions on the flow of a micropolar nanofluid via a wedge was inspected by Zulkifli et al. [17]. The impact of chemical processes on the thermal energy and mass transport flows of a magneto-micropolar fluid through a non-conducting wedge containing Hall and Ion-slip currents was inspected by Singh et al. [18]. The Soret and Dufour influences on the heat transport processes of micropolar fluids on a thick needle travelling in a parallel flow were numerically explored by Maboob et al. [19]. Falkner and Skan [20] explored the issue of boundary-layer flow on a wedge for the first time, introducing suitable transforms identified as Falkner-Skan solutions that may be used to fluids with like flows to convert differential boundary-layer equations to ODEs. After that, Hartree [21] examined the Falkner-Skan flow problem quantitatively. The concept of non-Newtonian (micropolar) fluid flow around the wedge, as addressed in the paper, is undoubtedly a fascinating issue to consider because the fluid might refer to a variety of fluid types with complex properties that are not explained by Newtonian fluid. Many sectors of engineering and science use heat exchange and boundary layer flow across a wedge-shaped body. Elbashbeshy et al. [22] researched the heat

exchange flow on the wedge surface. Xenos et al. [23] evaluated the influence of turbulent flow on a wedge surface. For a range of physical processes, several writers [24–30] explored fluid flow and heat movement in surface wedges.

In many physical models, heat transport through a heat source/sink is the most notable element. When there is a considerable thermal energy variation between the surrounding fluid and the surface, the influence of heat creation (source) or absorption (sink) seems to be quite substantial. The heat source, which is often dependent on temperature and space, has a noticeable impact on the fluid's heat transmission capabilities. Controlling heat transfer is greatly influenced by the heat source/sink. Tufail et al. [31] employed Lie group analysis to find similarity results for non-Newtonian flow with a magnetic-intensity and a heat source or sink involving a magnetic intensity. The flow of non-Newtonian nanofluids with magnetic flux and a heat sink/source was studied by Ramesh et al. [32]. Pal [33] looked into how fluid flow, which is dependent on time, on a strained surface including an uneven heat sink or source affected thermal transfer. Kumar et al. [34] examined the heat exchange properties of ferrofluid flow across a convective sheet containing radiation. Mabood et al. [35] researched the impact of a changing heat source and sink on the flow of micropolar fluid over a stretched sheet including thermo-diffusion. Makinde et al. [36] and Mabood et al. [37] investigated the effects of heat source or sink, and radiation on the nanofluid flow over a non-linear surface and came to the conclusion that the heat sink factor tends to raise temperatures. The fully formed thermal energy and mass transport of a micropolar liquid through a upright channel including a heat source and sink is explored by Umavathi et al. [38]. Many scholars, such as [39–45], have looked into the significance of non-uniform heat sink or source affects in many forms of flows.

Microorganisms like bacteria and microalgae are heavier than water and so have the ability to travel in the reverse direction of gravity. The density of the topmost layer of suspension gets so large as a result of the conglomeration of microorganisms that the density distribution in the suspension’s bottom layer becomes unstable. Hence, convective instability develops, and convection patterns begin to form. Bioconvection is the term for the voluntary and random movement of microorganisms. Many researchers have studied this phenomenon because of its practical uses in commercial, industrial, and environmental items such as ethanol, fertilisers, and fuels. Bioconvection is a macroscopic convective motion caused by the correlated movement of motile microorganisms in fluid. Because microorganisms are denser than fluid, their movement causes a rise in fluid density. This happens because of upward self-derived motion, which causes a stratified layer to emerge on the upper portion of the fluid. The combined convected micropolar nanofluid flow with magnetic flux, energy of activation, and gyrotactic microorganisms is described by Waqas et al. [46]. As per the existing/available literature, the improved micropolar fluid including gyrotactic microorganisms has received less attention than the critical engineering and industrial applications. Kuznetsov et al. [47-48] have visualised several recent achievements in this field.

The bioconvective Carreau nanofluid flow with a magnetic effect on thermal radiation and velocity slip is studied by Muhammad et al. [49]. The outcomes of several fluid models, such as Newtonian, micropolar, Williamson, and Maxwell, for mass and heat transfer due to expanding surfaces, including microorganisms, are compared by Habib et al. [50]. Song et al.[51] investigated the bioconvection flow of the Brinkman form of micropolar fluid related to an extending inclined surface when there was liquefying thermal performance. Khan et al.[52] have studied magnetised micropolar fluid flows, including motile microorganisms with changeable heat conductivity travelling across a moving surface. A biconvection study of micropolar fluid flow containing microorganisms with activation energy was studied by Abdelmalek et al. [53]. The flow of 2-D Casson nanofluid across a wedge having swimming and motile microorganisms with heat and activation emission has been examined by Waqas et al. [54].

The true purpose of this topic, which is motivated by the above literature, is to investigate biconvective micropolar fluid flow with heat source/sink and material properties over a wedge. In the fluid modelling, the Eckert number and the FalknerSkan parameter are taken into account. Based on the above literature assessment, it appears that the impact of gyrotactic microorganisms on micropolar fluid flow receives less attention. Several essential features have shown a negligible effect on secondary velocity. Nanotechnology, biotechnology, food industries, cancer therapy, polymer coating systems and a wide range of other industries etc. can all benefit from the existing approach.

1. Problem formulation

We take into account the 2-D forced convective fluid flow over a wedge that is incompressible, steady, and contains motile microorganisms. The authors utilize rectangular coordinates (x y z, ,) , where x , y , and z correspond to measurements along the wedge, normal to the topside of the wedge, and in the direction of wedge's main edge, respectively. The wedge lies in the xy □ *plane*, where the fluid flow is in the direction of the x -axis. As shown in Fig. 1, the wedge is positioned so that its surface lines up with the x -axis and the y -axis is vertical to it. The xy □ plane is perpendicular to the z -axis. Fluid flow is thought to be created by extending a wedge at a velocity of U in the current investigation. Assume the exterior velocity of the wedge is$U$ x cx( ) □ ^{m} , here c - is the positive constant, m □□ □* / 2□ □ *□ , wedge parameter with 0 □ □m 1, □ □* □□/ . The flow is decelerated (retardation) for□* □ 0, whereas it accelerates for □* □ 0, and□* □ 0 correspond horizontal flat plate to fluid flow. To make the problem easier to understand, the authors assume that the flow and heat transport amounts in the z □*axis* do not change.

Axisymmetric

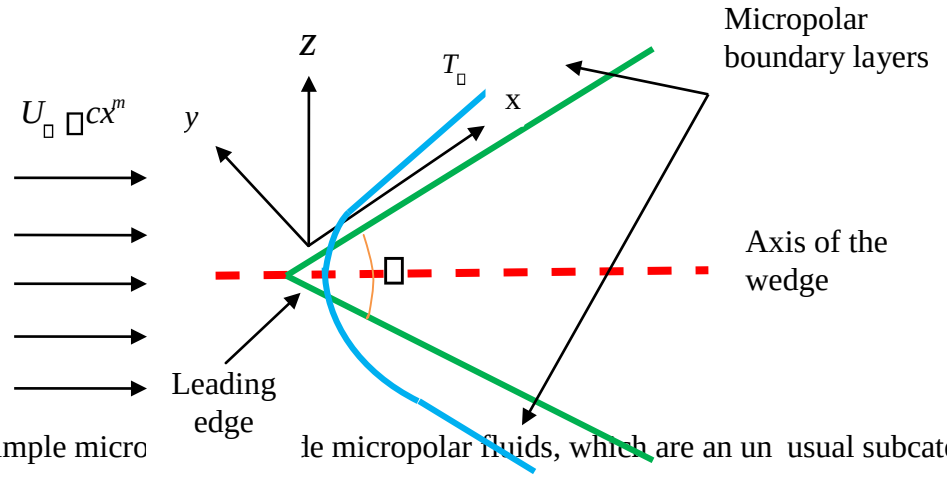

Simple micro le micropolar fluids, which are an un usual subcategory. Local movements of physical particles present in everyT_{w} of the volume element, i.e.

Figure 1. Physical model

microelement, influence the behaviour and properties of these fluids, and thus have local inertia. Volume elements in micropolar fluids comprise hard (non-deformable) particles that can spin around the volume element's centre and are described by a microrotation vector. The customary stiff body movement of the full volume element, that describes N-S fluids, is supplemented with this local movement of the particles. Thus, supplementary equations that consider the conservation of micro-inertia moments and the balancing of initial stress moments, both of which emerge as a result of the study of microstructure in a fluid, are added to the classical continuum laws in the mechanics of micropolar fluid. As a result, classical (continuity of) fluid dynamics theory is combined with novel

kinematic variables, as well as ideas of stress moments, and microstress. For micropolar fluids, the field equations in vector form are as follows [7, 56]:

Mass conservation

$$\frac{\partial \rho}{\partial t} + \nabla \cdot (\rho V) = 0 \quad (1)$$

Translational momentum conservation

$$\rho \frac{dV}{dt} = -\nabla p + \mu \nabla^2 V + \kappa (\nabla \times G) + \rho f \quad (2)$$

Rotational momentum (micro-rotation) conservation

$$\rho I \frac{dG}{dt} = \phi \nabla (\nabla \cdot G) + \gamma \nabla^2 G + \kappa (\nabla \times V) - 2\kappa G + \rho l \quad (3)$$

The velocity (known from the N-S hypothesis) and the axial vector field, which mimics the spin of the micropolar fluid molecules, are the only two distinct kinematical vector fields that we are concerned with in the theory of the micropolar models. These are supposed to be rigid. We should remark that in micropolar fluid theory, there are no external body forces in which the fluid has fixed physical characteristics, and the conservation equations for steady state flow are considerably reduced. Furthermore, when $\kappa = 0$ and l , f are vanishing, the gyration vector vanishes, and eqn. (3) disappears completely. In this exceptional instance, equation (2) also simplifies to the traditional N-S Eqs. The momentum vector V and the microrotation G are uncoupled when $K = 0$ only, and the global movement is not affected by the microrotations. For the axisymmetric wedge problem with a fixed thermal flux on the wedge surface, this model was used. The ambient fluid's temperature (T_∞) (free stream) is considered to be stable. The equation for the micropolar fluid system including motile bacteria is: Continuity,

$$\frac{\partial u}{\partial x} + \frac{\partial v}{\partial y} = 0 \quad (4)$$

Linear (translational) momentum conservation along x axis:

$$\rho\left(u\frac{\partial u}{\partial x} + v\frac{\partial u}{\partial y}\right) = \mu\frac{\partial^2 u}{\partial y^2} + \kappa\frac{\partial N}{\partial y} + \rho U\frac{dU}{dx} \quad (5)$$

Linear (translational) momentum conservation along z axis

$$\rho\left(u\frac{\partial w}{\partial x} + v\frac{\partial w}{\partial y}\right) = \mu\frac{\partial^2 w}{\partial y^2} \quad (6)$$

Angular momentum (microrotaion) conservation

$$\rho j\left(u\frac{\partial N}{\partial x} + v\frac{\partial N}{\partial y}\right) = \gamma\frac{\partial^2 N}{\partial y^2} + \kappa\left(2N + \frac{\partial u}{\partial y}\right) \quad (7)$$

Energy conservation

$$\rho C_p\left(u\frac{\partial T}{\partial x} + v\frac{\partial T}{\partial y}\right) = k\frac{\partial^2 T}{\partial y^2} + \mu\left(\frac{\partial u}{\partial y}\right)^2 + \kappa\left(\frac{\partial w}{\partial y}\right)^2 + Q(T - T_\infty) \quad (8)$$

Density of gyrotactic microorganism

$$u\frac{\partial M}{\partial x} + v\frac{\partial M}{\partial y} + \frac{bW_c}{\Delta C}\left[\frac{\partial}{\partial y}\left(M\frac{\partial C}{\partial y}\right)\right] = D_m\left(\frac{\partial^2 M}{\partial x^2} + \frac{\partial^2 M}{\partial y^2}\right) \quad (9)$$

Where □ □□□□□ □□□_2 □□□ *j* . The relevant boundary constraints are given on the wedge surface and at the boundary layer regimes border on the stream (far off the wedge).

They are of the following kind:

$$u \square 0 , v \square 0, w \square 0 , N \square\square n\_\_\_^{\square u}, q_w \square\square k\_\_\_^{\square T} , M M\square_w \text{ when } y \square 0 \qquad (10a)$$

$$\square y \qquad \square y$$

$$u \square \square U \qquad cx^m; w\square 0, N \square 0, T \square T_\square, M \square M_\square \quad \text{as } y \square\square \qquad (10b)$$

The parameter *m* in equation (10b) has multiple significant values that correspond to traditional flow configurations. There are four situations worth mentioning:

Case 1: When □*is in the interval(0,2) , this means*m*□ 0, the flow is a generalised 2-D wedge flow.

Case 2: When□* □ 0, for which*m*□ 0, on a horizontal, flat plate that is partially infinite, fluid flows.

Case 3: Forward stagnation point flow close to the upright surface happens when □* □1implies*m*□1.

Case 4: Rear stagnation-point flow close to the vertical surface happens when □* □□1 that implies*m*□□1/3.

The starting three scenarios are the most essential to polymeric coatings. When it comes to heat transport, these scenarios are also completely valid. The micro-rotation border restrictions, which are governed by the value of *n* in (10a), permit for a wide range of physical possibilities to be investigated. In this scenario, we will use*n*□ 0.5 , that relates to a low micro-element concentration near the wall. The situations *n*□ 0 and *n*□1are linked with significant at the wall concentration and turbulent flows, respectively, but none of these are pertinent in our study. As a result, the micropolar fluid model includes a separate angular momentum balance together with additional boundary requirements/constraints. Considering Equations (5) and (7) implies a strong connection amidst the angular momentum and primary translational momentum profiles, despite the absence of partial derivatives, as in previous visco-elastic model's. Solving the parabolic PDE's (4)–(9) remains a difficult task. Consequently, the boundary value issue can be transformed to produce more numerically tractable solutions. As a result, we establish the scaling transformations and non-dimensional variables below, as well as a stream function□, given by $u_\square$ ___ □□ and v □□___ □□, that effortlessly follows mass

$$\square y \qquad \square x$$

conservation:

$$\_\_\_\_\_ \qquad \_\_\_\_\_ \quad \square\square\square\square\square m\square 1\square U \square\square 1/2 \qquad \square\ 2\square xU\ \square 1/2\ F(\ )\square\ , \qquad w$$

□*UG*□□□ ,

y , □□□

$$\square \quad 2\square x \square \qquad \square\ m\square 1\ \square\square$$

$$\square\square m\square 1\square U \square^{1/2} \qquad k\ T\ T\square\ \square\ \square\square\square m\square 1\square U \square^{1/2}$$

$$N\ UH\square\square\square\square\square\_\_\_\_\_\square , \qquad \square\square\square\ \square\square\_\_\_\_\_\square\_\_\_\_\_\ \square ,$$

$$\square \quad 2\square x \square \qquad\qquad qw \quad \square \quad 2\square x \square$$

$$2xQ\ x(\ ) \qquad \square \qquad \square^2 \mathrm{Re}$$

$$\square\square \ \_\_\_\_\_ , \quad K \square \qquad \_ , \quad \frac{I \square}{j \dfrac{U^2}{\_\_\_\_\_}} \qquad (11)$$

$$\square C\ U_p \qquad \square$$

C_p □*T* □$T_\square$□

Utilizing equations (11), the Eqs. (4–8) are simplified to the coupled set of nonlinear equations that are listed below:

Primary momentum

$$\square 1\square\ K\ F\square\ '''\square\ K\ H\ '\square\ F\ F\ ''\square^{\square}\square\ \_\_\_\_\__m^{2m}\square_1\square^{\square}\square\square 1\square F\ '^{\,2}\square\square\ 0 \qquad (12)\ \square$$

Secondary momentum

$$\square 1\square K\,G\square\ "\square\ \square\ \square\ \_\_\_\__{m}^{2m}{}_{\square 1\square}\square\ \square F\,G'\ \square\ FG'\ \square\ 0 \qquad (13)$$

Angular momentum

$$\square\square 1\square\ \_\ K2\ \square\square\square H\ "\square\square\square\square\square\square\square\ \_\_\_\_\_\ 3mm\square\square 11\square\square\square F\ \ H'\ \square F\ \ H\ '\square\square\square\square\square\square\square\ \_\_\_\_$$

$$m2KI\square 1\square\square\square\square F\ "\square\ 2H\square\square\ 0 \qquad (14)\ \square$$

Energy,

$$\square\square\square\ \_\_\_\_m\mathrm{Pr}\square 1\square\square\square\square"\square\square m\square 1\square F\ '\square\square\ \square\square 1\ K\square\square m\square 1\square Ec\ F\square\ "\ 2\square G\ '\ 2\ \square\square$$

$$\square\square\ \square\ \square\square\ \square m\ 1\square F\square'\ \square\ 0 \qquad (15)$$

Density,

2

$$\square\square$$

$$\square_{\square}\square\square m\square\quad 2\sqrt{\frac{m\ \square 1}{2}}\quad \square 1\square\mathrm{Re}\square_{\square}\ \square\ \square"\square\ \square m\ m\square 1\square\square\ \square 3\square\square'$$

$$\square\square$$

$$\square\square$$

$$\square\square_{\square}\quad \sqrt{\frac{m\ \square 1}{2}}\quad 4\square m\square 1\square\mathrm{Re}\ \square\ 2\ Lb\ \mathrm{Re}\square m\square 1\square F\square_{\square}\ \square'\ \square\ 0 \qquad (16)$$

$$\square\square$$

The relevant converted boundary restrictions are ascertained as:

$F(0)\ \square\ 0\ ,\quad F\ '(0)\ \square\ 0\ ,\quad G(0)\ \square\ 0\ ,\quad H\ (0)\ \square\square nF\ "(0)\ \ ,$

$\square'(0)\ \square\square 1,\quad \square(0)\ \square\ 1\quad \text{at}\quad \square\square\ 0$

$$F\ '(\square\ \square)1,\ G(\square\ \square)\ 0,\ H\ (\square\ \square)0,\ \square(\square\ \square)0\ ,\ \square(\square\ \square)\ 0\ \text{as}\ \square\square\square \qquad (17)$$

2. Physical quantities

We are keen in the momentum, micro-rotation, temperature, and density of microorganisms in engineering computations, as are a few of their gradient functions.

The primary and secondary dimensional wall shear stresses are expressed in the form:

The primary friction drag is as follows:

$$2\square x \qquad \_\_\_\_$$

$$Cf\,x\ \square\ U2\ \square$$

The secondary friction drag is as follows:

$$2\square w\ Cf\,z\ \square\ U\ 2\ \square \qquad \_\_\_\_$$

The following formula is used to determine the wall couple stress:

$$Cw\ \square\ cwU^{\square}32 \qquad \_\_\_\_$$

$$\square$$

The dimensional Nusselt number is calculated as follows:

$$N_u\ \square\ k\ T\square\ \square T_{\square}\square \qquad \frac{xqw}{\_\_\_\_\_}$$

The dimensional local microorganisms number can be calculated as follows:

$$\mathrm{Mn}\ \square\ D_m\ \square M_w\ \square M_{\square}\square \qquad \frac{xqn}{\_\_\_\_\_}$$

Where $\square x\ \square\ \_\_\_\_\ U2\ \ 2\ \_\_\ \square\square\square\ \ \square\square\ \ \square\square uy\ \_\_\ \square\square N\square\square\square y\square 0\ ,\ \square\ \ \square\ \ \square w\ \square\square\square\square\ \ \square\square\square wy\ \square\square\square y\square 0\ ,$

$$c_w\ \square_{\square}{}^{\square N}\ \_\_\ \frac{\square\ \square}{\square y}\Big|_{y\square 0}\ ,q_w\ \_\_\ \frac{\square}{\square y}\square\square k^{\square T}\Big|_{y\ \square\ 0},\ \_\_\ \frac{}{\square y}\ q_n\ \square\square D_m{}^{\square M}\ \_\_\ \frac{}{\square}\Big|_{y\ \square\ 0}\ \text{and}\ \ \mathrm{Re}\ \square\ {}^{U\,x}$$

The following are the physical quantities in dimensionless form:

$C_{fx}\,\mathrm{Re}^{1/2} = 2(m+1)^{\frac{1}{2}}\left[1+\frac{K}{2}\right]F''(0)$,

$C_{fz}\,\mathrm{Re}^{1/2} = 2\left(\frac{m+1}{2}\right)^{\frac{1}{2}}\left[1+\frac{K}{2}\right]G'(0)$, $C_w\,\mathrm{Re}^{\frac{m+1}{2}} = H'(0)$,

$Nu\,\mathrm{Re}^{-1/2} = \sqrt{\frac{m+1}{2}}\,\theta'(0)$, $Mn\,\mathrm{Re}^{-1/2} = \sqrt{\frac{m+1}{2}}\,\chi'(0)$ (18)

It is worth noting that the gradients $F''(0)$, $G'(0)$, and $H'(0)$ can be used to investigate skin frictions, wall couple stress, heat exchange rate, and local microorganisms number. The current flow model has a number of pertinent special situations. Newtonian convection is described by the flow model as $K = 0$. Viscous heating is prohibited when $Ec = 0$ and there is no heat sink when $\theta = 0$. When $m = 0$, the flow on the wedge transforms into Blasius flow through a flat plate. When $m = 1$, the example of flow near a stagnation point on an unending plate is recalled.

3. Results and Discussion

An extensive number of computations are carried out with different parameter values to understand the nature of primary velocity, angular velocity, temperature and motile microorganisms and are displayed in Figures 2 – 6. The default parameters chosen are $I = 0.5$, $K = 0.5$, $m = 1/3$, $\mathrm{Pr} = 100$, $\gamma = 0.5$, $Ec = 0.2$ and $Lb = 1.0$.

Figs. 2a – d explain the impact of pressure gradient factor (m) on $f'(\eta)$, $H(\eta)$, $\theta(\eta)$ and $\chi(\eta)$ respectively. As stated before, for $m = 0$, Case-II acquired, i.e., flow through a semi-infinite horizontal plane also called Blasius flow. When m is equal to one, Case-III is retrieved, i.e., forward stagnation-point flow ($\beta = 180^0$'s) close to a upright surface. The indeterminate situation, i.e., $m = 1/3$ (wedge), $m = 0.7$ (wedge), corresponds to $\beta = 90^0$'s and $\beta = 148^0$'s, respectively. The last situation consequently suggests a very sharp wedge shape. Fig. 2a demonstrates that when m grows, the horizontal velocity rises and the width of the velocity boundary layer falls. This is because increasing m results in the progression of velocity over the wall and hikes the increase of the boundary layer. The vastness of the momentum is peak for values of $m = 0$ and the optimal velocity is obtained with $m = 1.0$. Further the momentum is minimal for the Blasius flow ($m = 0$). Hence one can conclude that steeper the wedge geometry higher the horizontal velocity. Again, an asymptotically smooth profile is calculated in the free flow, which confirms the existence of a large enough infinite boundary in the free flow. The similar observations were identified in reference [55] for the nanofluid flowing past a wedge for a Newtonian fluid.

Fig. 2b illustrate the variation in secondary velocity $H(\eta)$ with m near the wedge surface as m increases the angular velocity decreases suggesting that there microelements rotate progressively in the opposite direction. Hence there is angular deceleration owing to the increasing reverse spin. This nature occurs in the range $0 \le \eta \le 1$ and for values of $\eta > 1$, there is an acceleration in the angular velocity and sustained into the free stream. Peak values of $H(\eta)$ arise in the Blasius flow example ($m = 0$) and are progressively with growing values of parameter m. For $m = 1$, smooth increase in $H(\eta)$ occurs from the boundary to the unrestricted flow. However, for $m = 1.0$ a specific monotonic increase occurs from the leading edge to the unrestricted flow. For all values of m, the asymptotically smooth profiles converge at $\eta = 3.0$. The rotary movements of the micro-elements are thus significantly influenced by the wedge parameter.

Fig. 2c shows the influence of m on temperature $\theta(\eta)$. Increasing m clearly increases temperature, with the biggest change occurring away from the wedge surface. Therefore, a bigger wedge parameter causes the thickness of the thermal boundary layer to grow. In comparison to the Blasius flat plate example ($m = 0$), a higher heating regime is created for the forward stagnation flow scenario ($m = 1.0$), with the wedge case coming in between these two ends.

Fig. 2d displays the effect of m on□□( ) . Increasing m increases □□( ) near the leading edge and the profiles converge in the free stream for all values of$m$. The motile density boundary layer thickness therefore rises with larger wedge parameter. The □□( ) is maximum for m□1.0 and minimal for$m$□ 0. m arises in each term of equation (16), as m is a function of □*and its effect is dominant in primary and angular momentum fields rather than □□( ) . The □□( ) attains the peak via forwarded stagnation scenario rather than any other geometrical case, although, (Fig. 4), heat sink (□) has a considerably more significant impact and generates a lot stronger cooling. Fig. 3a – d elucidate the implication of material parameter (K) on the functions F '□□□, H □□□, □□□ □, and □□( ) for m□1/3 . A significant deceleration in primary flow (Fig. 3a) is caused, that is in contrast to the traditional responsiveness in the horizontal surface boundary layer flow, as stated by Beg et al. [56], Gupta et al. [57] and Nath [58], amongst other. The normal impact of micropolar fluids on reducing drag in horizontal plate flows cannot be realised in wedge flows because the primary velocity is reduced. Furthermore, regardless of the Eringen parameter's value, no backflow is produced, and primary velocity computations result in dependably smooth climbs from the wedge surface to the liberate stream. Maximum acceleration is attained in the Newtonian fluid scenario (K □ 0), and greatest deceleration is attained in the highly micropolar case (K □ 2). Clearly, the revised shear term, i.e., (1□ K) $\frac{d^3 F}{d}$□3 and the coupled factor, K $\frac{dH}{}$, which features the Eringen Micropolar factor, generate d□ significant changes in the primary velocity field. Therefore, the width of the border layer of the primary velocity is augmented with Eringen micropolar vortex viscosity, i.e., higher values of K .

Fig. 3b shows that there is an increase in angular velocity near the wedge surface in the range of 0 □ □□ 1.2 . However, quickly this pattern is reversed and there is a robust deceleration induced in angular momentum with increasing vortex viscosity and then the profiles merge in the free stream. The rotary motions are damped away from the wedge surface whereas they are boosted near the wedge surface. Fig. 3c promotes the temperature field with increasing the vortex viscosity parameter K . The Newtonian fluid shows the cooling effect in comparison with the Micropolar fluid. Fig. 3d also shows the similar effect on □□( ) as that of □□( ) but the magnitude is different. The function□□( ) is not much deteriorated with K .

Fig. 4 shows the progression of temperature with □, in the scenario of m□1/3 (allinclusive wedge movement). The wedge example above relates to a wedge angle of nearly90^0, i.e., a steep (perpendicular) wedge geometry. For□□□1, monotonic declines into the free flow are seen, and the highest temperature is calculated on the wedge surface (wall) in each profile. A kink develops in the zone close to the wall for the case □□ 2.0, and a feeble climb thereafter takes place to the free flow. The removal of more thermal energy from the boundary layer through the wall is implied by a stronger heat sink. As previously mentioned, this method is employed in the production of polymers to avoid the additional heat build up caused by viscous dissipation. As a result, manufactured items produce a more homogenous thermal diffusion and have a stronger heat sink effect, which greatly reduces the temperature boundary layer width. Higher temperatures, that are undesirable in processes involving the processing of materials, would undoubtedly ensue from the absence of a heat sink □□□ [59, 60]. In these flows, a heat source □□□ 0□ is similarly unsuited for thermal regulation; hence it is not taken into account in this context.

Fig. 5 shows how the viscous heating factors, $Ec\ u\ c\ T$□ ^{2}/ □ effect on temperature (□□( )) changes. Viscous heating has a considerable impact on the flow of polymer coatings. As discovered by Winter [61], a part of the work of deformation is transformed into thermal energy by internal drag when a very sticky liquid (such as

polycarbonate mixture) is distorted in a fluid domain. The large value (Pr □100) is assigned to the Prandtl number. Because of this, the thermal diffusivity in the flow is significantly higher than the kinematic viscosity, and the heat conductance is likewise too much lower. In other words, heat is convicted more slowly than momentum. According to the expression (1□ *K Ec F*) □ " ^{2}□*G* ' ^{2}□ in the temperature border layer eqn.
15, this amplifies the contributions of the primary and secondary shear rates. When
Ec□ 0 , viscous dissipation impacts are denied, and temperatures are reduced. The implication is that the temperature field is under-predicted when viscous heating is ignored. Rising values of *Ec* (which correlates the boundary layer enthalpy difference to the K. E. lost in the flows) leads to hike in the thermal boundary layer thickness. Another thing to keep in mind is that the primary and secondary contributions to viscous dissipation are both taken into account in the current research, but in the great part of research published in the existing work, exclusively the primary momentum contribution is factored into models.
Fig. 6 depicts the effect of bioconvective Lewis number on motile microorganism density function (□□( )). At the wall, □□( ) is large and equal for any value of *Lb*and falls down in the range 0 □ □□ 0.6 . For *Lb*□ 0.6all profiles converges and remains constant towards the free stream. Physically, for larger *Lb* values, the diffusion coefficient of microorganisms' decreases and thus the locomotive denseness degrades.
The validation of the results have been carried out and depicted in table-1 with the published work [62, 63, 64]. This table shows that the current outcomes agree very well with the earlier published research. The influence of *m* , *K* , *I* and *Lb*parameters on the wall primary stress, rotational momentum gradient, local heat transport rate, and local density number of motile microorganisms is shown in table-2.The growth in the value of *m* reveals the increasing impact on shear stress, couple stress, and local Nusselt number. For*m*□1, i.e., in the forward stagnation point flow (□□ 180^0s) the motile microorganism number drops but shows increasing behavior for acute wedge. The motile microorganism number has dropped for*m*□1, i.e. in the forward stagnation point flow (□□ 180^0), but improves for acute wedge angle. The impact of *K* on the couple stress, Nusselt and motile microorganisms' numbers diminishes, while the primary stress increases. Further, an increase in micro-inertia parameter raises local Nusselt number and reduces both shear stress, and couple stress but the local microorganisms number remains constant. The Lewis number of bioconvection has no impact on *F* "(0) , *H* '(0) , and □□'(0) . The increase in *Lb* shows an increasing effect on the motile microorganisms' numbers.

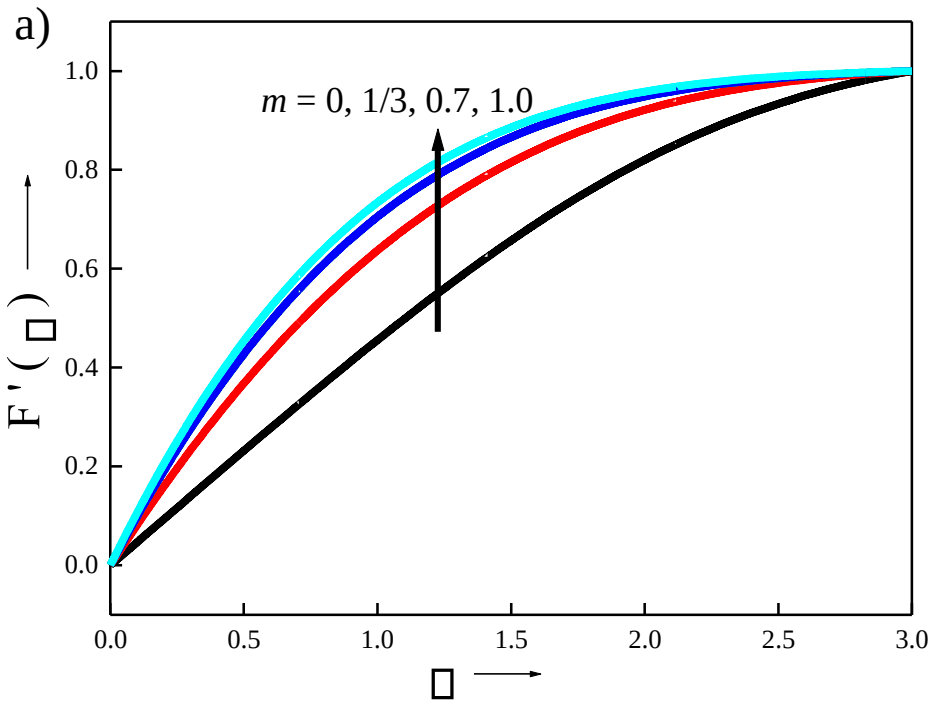
a)
m = 0, 1/3, 0.7, 1.0
F '( )
1.0
0.8
0.6
0.4
0.2
0.0
0.0
0.5
1.0
1.5
2.0
2.5
3.0

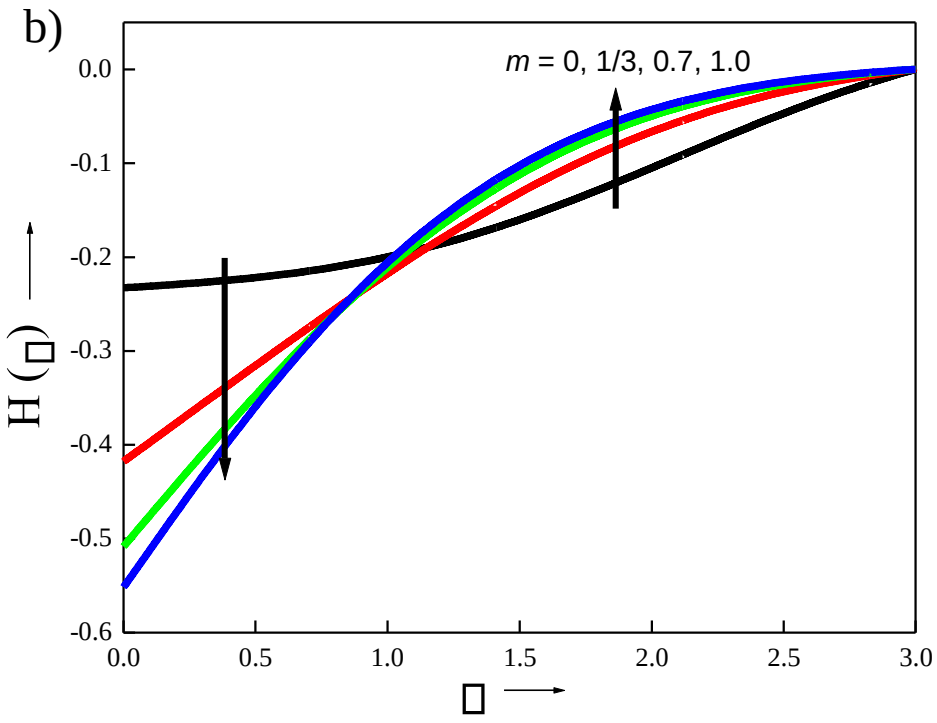
b)
m = 0, 1/3, 0.7, 1.0
H ( )
0.0
-0.1
-0.2
-0.3
-0.4
-0.5
-0.6
0.0
0.5
1.0
1.5
2.0
2.5
3.0

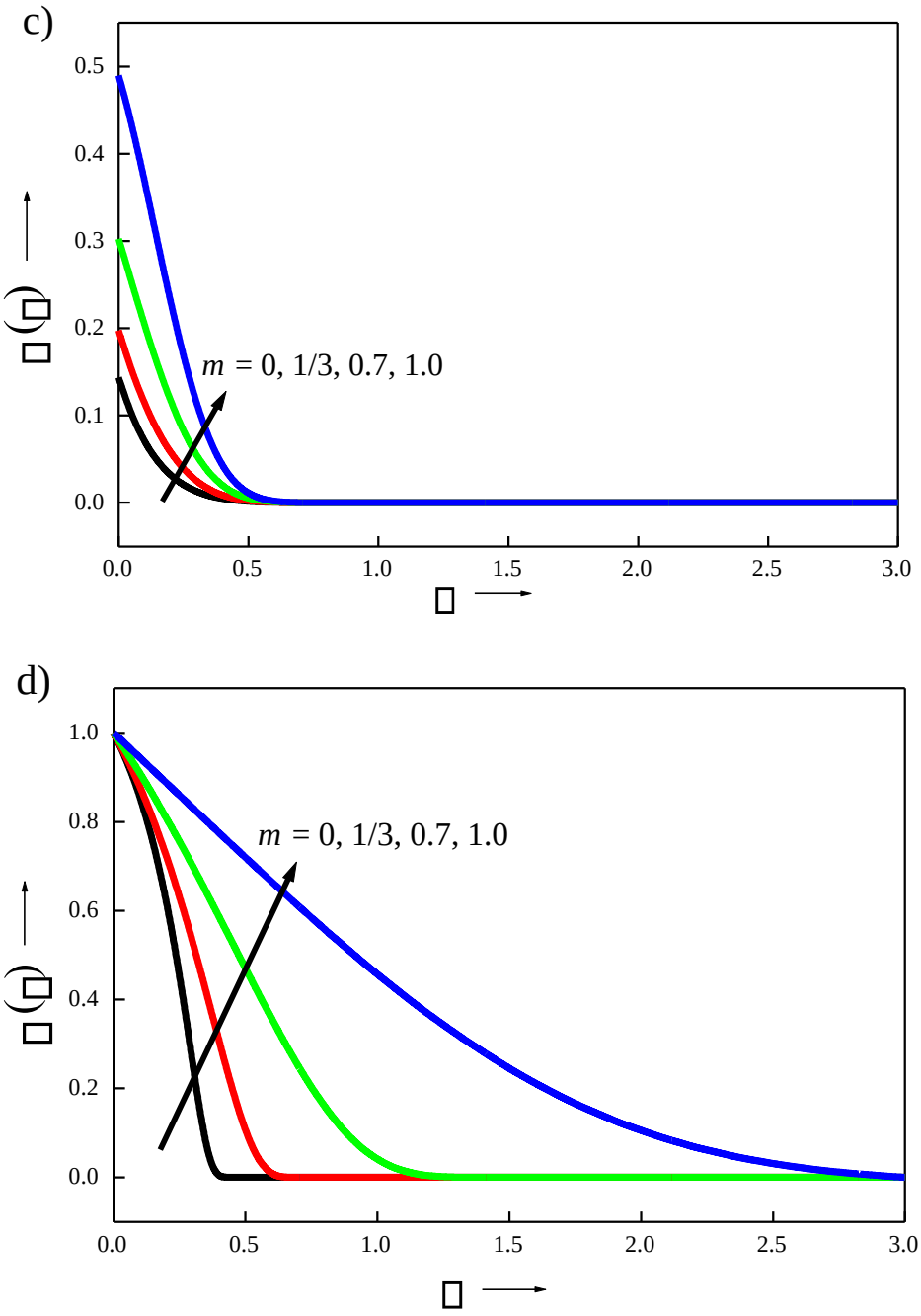

Figure 2. Profiles for **(a)** Primary velocity, **(b)** Angular velocity, **(c)** Temperature, **(d)** Motile microorganism versus pressure gradient parameter.

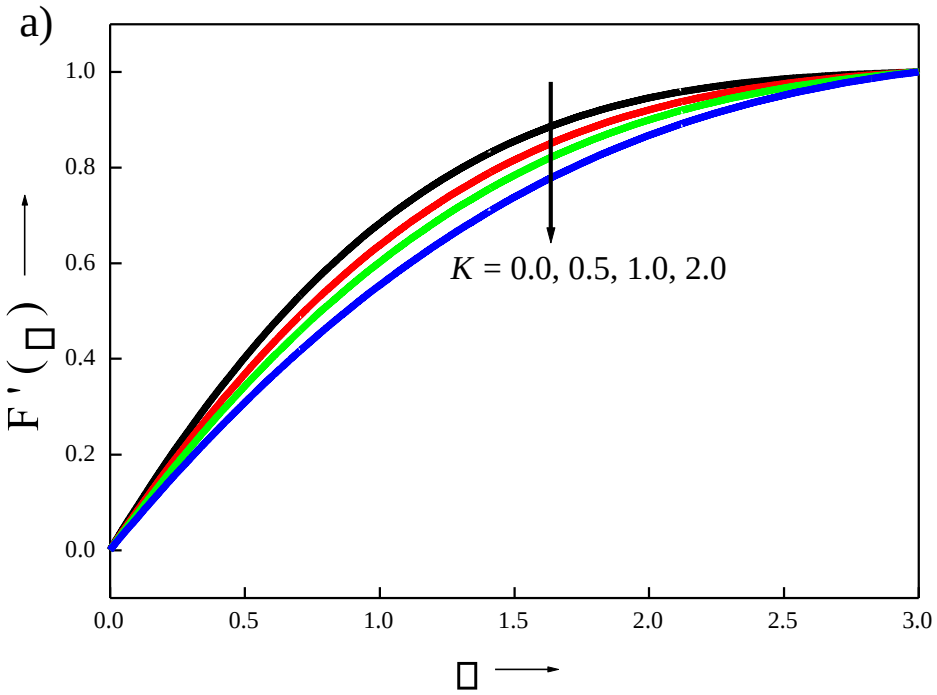
a)
1.0
0.8
0.6
0.4
0.2
0.0
F '(□)
0.0
0.5
1.0
1.5
2.0
2.5
3.0
□
K = 0.0, 0.5, 1.0, 2.0

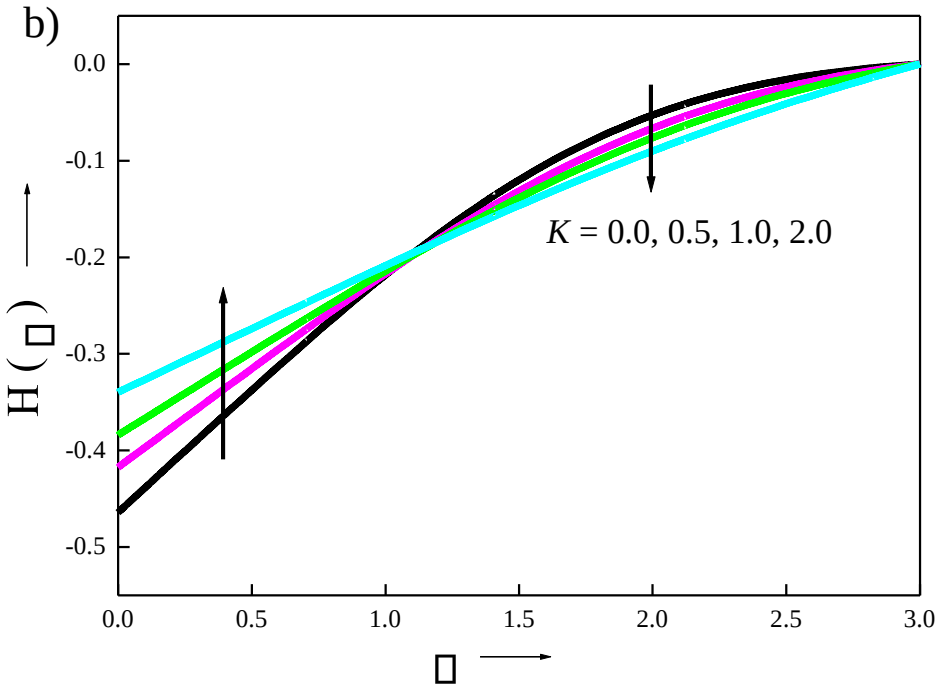
b)
0.0
-0.1
-0.2
-0.3
-0.4
-0.5
H (□)
0.0
0.5
1.0
1.5
2.0
2.5
3.0
□
K = 0.0, 0.5, 1.0, 2.0

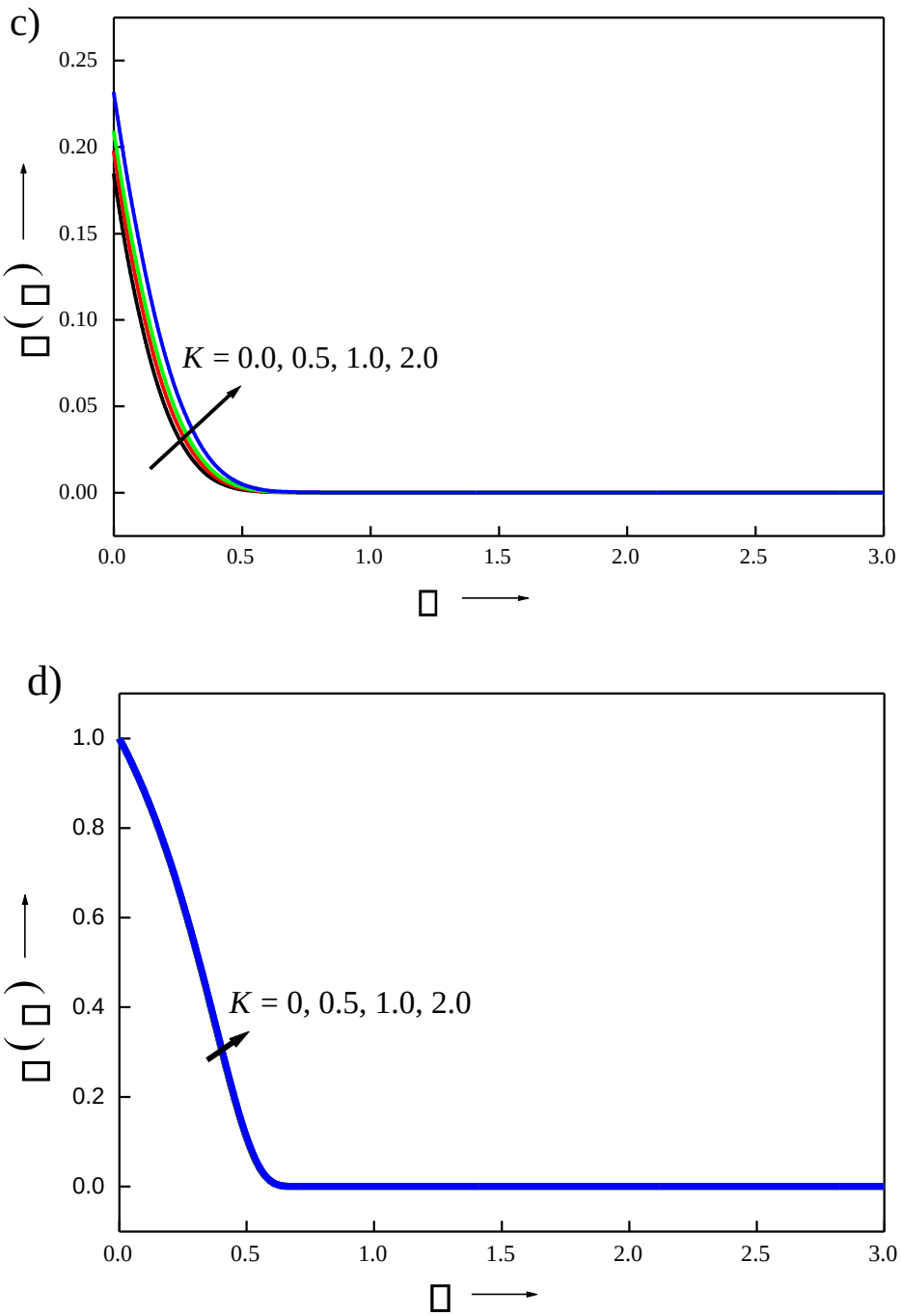

Figure 3. Profiles for **(a)** Primary velocity, **(b**) Angular velocity, **(c)** Temperature , and **(d)** Motile Microorganism versus vortex viscosity parameter.

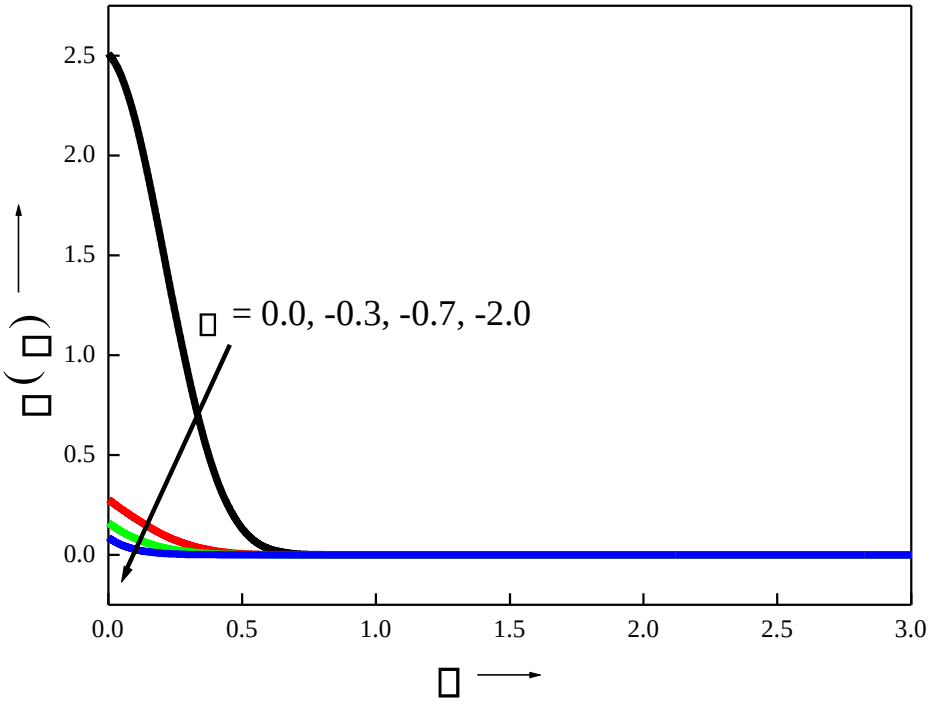

Figure 4. Profiles for temperature versus heat sink parameter.

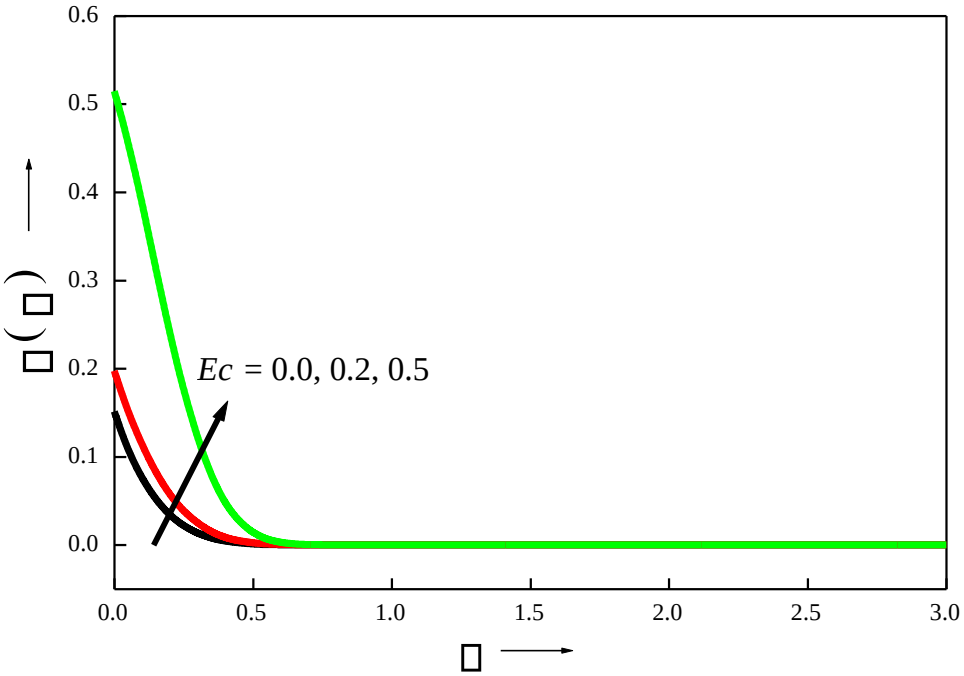

Figure 5. Profiles for temperature versus Eckert number.

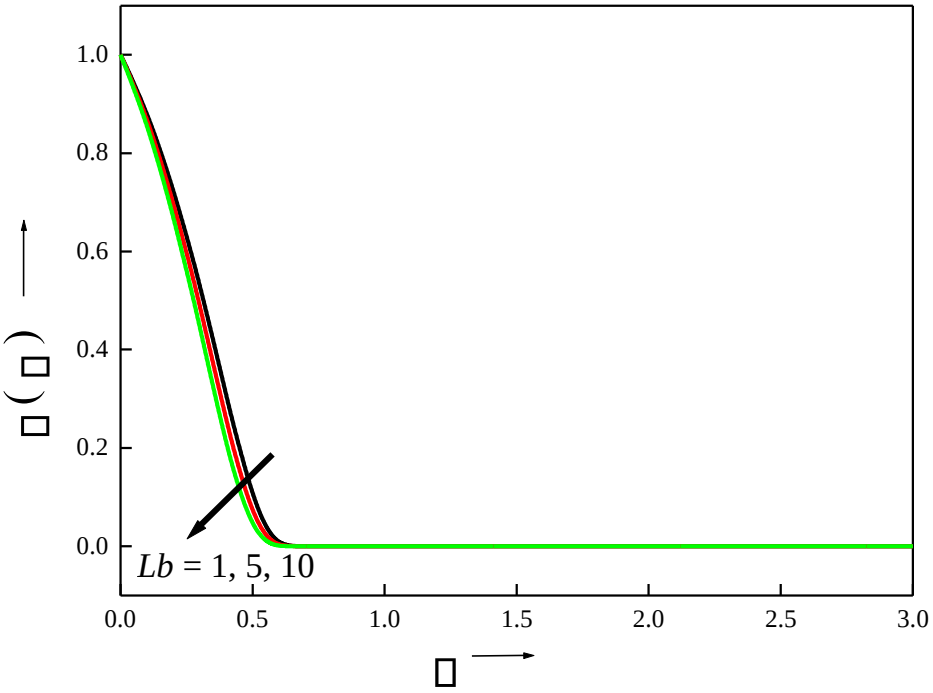

Figure 6. Profiles for density of motile micro-organism versus bioconvective Lewis number.

Table 1. Values of wall shear stress (skin friction coefficient) when K □ □m 0 for I □ 0.5, □□□0.5, Ec □ 0.2, Pr □100 .

K	m	Yih 62	Chamkha et al[63]	Ishak et al[64]	Present Result
0	0	0.332057	0.332206	0.332100	0.346600
0	1/3	0.757448	0.757586	0.757500	0.758600
0	1	1.232588	1.232710	1.232600	1.232815

Table 2. Values of F "(0) , H '(0) , □□'(0) , and □□'(0) , versus m , K , I and Lb.

m	K	I	Lb	$C_{fx}\sqrt{\mathrm{Re}}/2$	$C_w \mathrm{Re}$	$Nu/\sqrt{\mathrm{Re}}$	$Mn/\sqrt{\mathrm{Re}}$
0				0.4114	0.0089	4.9177	0.7972
1/3				0.8528	0.1366	4.1292	0.8665
1.0				1.3797	0.4016	2.0435	0.5640
	0			0.7586	0.1697	4.4246	0.8688
	0.5			0.8528	0.1366	4.1292	0.8665
	1.0			0.9415	0.1148	3.8972	0.8648
		0		0.8536	0.1393	4.1271	0.8665
		0.1		0.8534	0.1386	4.1276	0.8665

		0.5		0.8528	0.1366	4.1292	0.8665
			1	0.8528	0.1366	4.1292	0.8665
			5	0.8528	0.1366	4.1292	0.9503
			10	0.8528	0.1366	4.1292	1.0402

Conclusion

Theoretical analysis of micropolar fluid flow across a wedge containing motile microorganisms has been introduced, including heat removal and sticky dissipation effects. Applying the MATLAB bvp4c tool, a non-dimensional ODE boundary value problem was resolved using the 4^{th} order RK-method. The important conclusions from the discussion that came before are as follows:

1. Primary velocity is augmented by the growing wedge parameter, whereas the vortex viscosity parameter shows the reverse effect.
2. Angular velocity is decreased near the wall versus m while it is increasing when □□1.0 . Further, Eringen viscosity parameter (K) shows the reverse effect.
3. Temperature is enhanced with increasing K values near the wedge surface in the region 0 □ □□ 0.5 and the temperature profiles converge to zero for □□ 0.55 and remains constant towards the free stream.
4. The temperature and the width of the thermal boundary layer are significantly lowered by the effect of the rising wall heat sink, which cools the regime and aids in controlling the temperature in the dynamics of the polymer coating.
5. Increasing m increases □□( ) at the leading edge, and the profiles come together in the free stream for all values of m .
6. Higher wedge parameter significantly lowers the Nusselt number, although the parameter I has little effect on it.
7. An enhancement in the values of bio-convection Lewis number improves M_n .
8. Primary drag force and rotational momentum gradient are both incremented with the growing$m$.
9. The wall couple stress, Nusselt and motile microorganism number are reduced with increasing Eringen viscosity parameter (K).

Nomenclature:

$u\ v\ w$, , : Translational velocity components.

$x\ y\ z$, , : Cartesian coordinates

c : Non-negative constant

C_{fx} : Dimensionless primary skin-friction

C_{fz} : Non-dimensional secondary skin-friction

C_p : Specific heat

C_w : Dimensionless wall couple stress c_w : Dimensional wall couple stress

D_m : Diffusivity of microorganisms

Ec : Eckert number f : Body force per unit mass vector

F : Non-dimensional stream function F' : Primary velocity

G : Dimensionless secondary velocity

$\bar{G}$: Angular velocity (micro-rotation) vector

H : Dimensionless angular velocity (microrotation)

I : non-dimensional micro-inertia density parameter j : Micro-inertia density
k : Thermal conductivity
K : Vortex viscosity parameter/material parameter l : Body couple per unit mass vector
L : Arbitrary scale length
Lb : Bio-convection Lewis number m : Falkner-Skan power law index M_n : Density number of microorganisms n : Constant
N : Angular velocity in the xy □plane
Nu : Nusselt number
P : Thermodynamic pressure Pr : Prandtl number Q : Heat sink parameter q_w : Surface heat flux q_n : Surface motile microorganisms flux
Re : Reynolds number
T : Temperature function
T_w : Temperature at the wedge
$T_□$: Temperature at free stream
U : External velocity
V : Translational velocity vector

Greek symbols

□□, : Spin gradient viscosity coefficients for micropolar fluids
□* : Hartree pressure gradient
□ : Eringen spin gradient viscosity
□ : Motile microorganisms function
□ : Heat sink parameter (negative)
□ : Similarity variable
□ : Vortex viscosity coefficient
□ : Eringen 2nd order viscosity coefficient
□ : Newtonian dynamic viscosity
□ : Kinematic viscosity
□ : Dimensionless temperature
□ : Mass density of micropolar fluid
□ : Wedge angle
□$_x$: Primary dimensional wall shear stress
□$_w$: Secondary dimensional wall shear stress

Subscripts w : Wall conditions
□ : Ambient conditions **Acknowledgements:**

References

Taseer, M., Sultan, Z. Waqas, A. H., Habib, D., Ellahi, R., Bioconvection flow of magnetized Carreau nanofluid under the influence of slip over a wedge with motile microorganisms. Journal of Thermal Analysis and Calorimetry 143, 2021, 945–957.

Zaib, A., Haq, R.U., ―Magnetohydrodynamics mixed convective flow driven through a static wedge including TiO2 nanomaterial with micropolar liquid:Similarity dual solutions via finite difference

method‖. Journal of Mechanical Engineering Science 0(0), 2019, pp. 1 – 13 DOI: 10.1177/0954406219851157.

Schowalter, W. R., ―Mechanics of Non-Newtonian Fluids,‖ Pergamon Press, New York, 1978.

Prasad, V. R., Gaffar, S. A., Bég, O. A. ―Heat and Mass Transfer of a Nanofluid from a Horizontal Cylinder to a Micropolar Fluid‖. Journal of Thermophysics and heat Transfer Vol. No. 2014, pp

Zaib, A., Haq, R. U., Sheikholeslami, M., Khan, U. ―Numerical analysis of effective Prandtl model on mixed convection flow of γAl2O3-H2O nanoliquids with micropolar liquid driven through wedge‖. Phys. Scr. in press, 2019, 1- 28. https://doi.org/10.1088/1402-4896/ab5558.

Modather, M., Rashad, A.M., Chamkha, A. J. ―An analytical study of MHD heat and mass transfer oscillatory flow of a micropolar fluid over a vertical permeable plate in a porous medium‖. Turkish J. Eng. Env. Sci. 33, 2009, 245 – 257. doi:10.3906/muh-0906-31.

Eringen, A. C., ―Theory of Micropolar Fluids,‖ Journal of Applied Mathematics and Mechanics, Vol. 16, 1966, pp. 1–18. doi: https:// doi.org /10.1512 /iumj.

1967 .16.16001.

Ariman, T. Turk, M. A., Sylvester, N.D., ―Microcontinuum fluid mechanics–a review‖, Int. J.Eng. Sci. 11 (1973) 905–930.

Takhar, H.S., Agarwal, R.S., Bhargava, R., Jain, S.,―Mixed convection flow of a micropolarfluid over a stretching sheet‖, Heat Mass Transf. 34, 1998) 213–219. [10]. Seddeek, M. A., ―Flow of a magneto – Micropolar fluid past a continuously moving plate‖, Phys. Lett. A, 306, 2003, pp. 255–257.

Ishak, A., R. Nazar, R., Pop, I., ―Boundary-layer flow of a micropolar fluid on a continuous moving or fixed surfaces, Can. J. Phys. 84 (2006) 399–410.

Ishak, A., Nazar, R., Pop, I., ―Heat transfer over a stretching surface with variable heat flux in micropolar fluids‖, Phy. Lett. A, 372, 2008, pp. 559–561. [13]. Nadeem, S., Hussain, M., Naz, M., ―MHD stagnation flow of a micropolar fluid through a porous medium‖, Meccanica, vol. 45, 2010, pp. 869–880.

Rosali, H., Ishak, A., Pop, I., ―Micropolar fluid flow towards a stretching/ shrinking sheet in a porous medium with suction‖, Int. Comm. Heat Mass Transf., vol., 39, 2012, pp. 826–829.

Das, K., ―Influence of thermophoresis and chemical reaction on MHD micropolar fluid flow with variable fluid properties‖. International Journal of Heat and Mass Transfer, Elsevier, vol., 55, 2012, pp. 7166–7174.

Eringen, A. C., ―Theory of Thermomicrofluids‖. J. Math. Anal. Appl. Vol. 38, 1972, pp. 480-496.

Zulkifli, S. N., Sarif, S. M., Salleh, M. Z., and Samsudin, A., ―Magnetohydrodynamic micropolar nanofluid flow over a wedge with chemical reaction‖. IOP Conf. Series: Materials Science and Engineering, vol. 991, 2020, pp. 012145, doi:10.1088/1757-899X/991/1/012145.

Khilap Singh, Manoj Kumar. ―Influence Of Chemical Reaction On MHD Boundary Layer Flow Of A Micropolar Fluid Over A Wedge With Hall And Ion-Slip Currents‖. International Journal of Engineering Papers, January 2018; 3 (1), pp. 1–9.

Fazle Mabood, Nayak, M. K., and Ali J. Chamkha, A. J., ―Heat transfer on the cross flow of micropolar fluids over a thin needle moving in a parallel stream influenced by binary chemical reaction and Arrhenius activation energy‖. Eur. Phys. J. Plus, vol. 134, 2019, pp. 427. DOI 10.1140/epjp/i2019-12716-9.

Falkner, V. M., and Skan, S.W. ―Solutions of the boundary-layer equations‖. The London, Eldinburgh and Dublin. Phylosophical magazine and Journal of science. Vol. 12. No. 80, 1931, pp. 865 – 896. Doi:10.1080/14786443109 461870.

Hartree, D. R., ―On an equation occurring in Falkner and Skan's approximate treatment of the equations of the boundary layer‖. In Proc. camb. Phil. Soc., Cambridge, UK, vol., 33, 1937, pp. 223-239.

Elbashbeshy, E. M. A, Dimian, M.F., ―Effect of radiation on the flow and heat transfer over a wedge with variable viscosity‖, Appl. Math. Comput. Vol. 132, 2002, pp. 445e454.

Xenos, M., Tzirtzilakis, E., Kafoussias, N., ―Methods of optimizing separation of compressible turbulent boundary – layer over a wedge with heat and mass transfer‖, Int. J. Heat Mass Tran. Vol. 52, (1e2), 2009, pp. 488e496.

Rahman,M.M., Eltayeb, I. A., ―Convective slip flow of rarefied fluids over a Wedge with thermal jump and variable transport properties‖, Int.J. Therm. Sci. Vol. 50, 2011, pp. 468e479.

Yih, K. A., ―MHD forced convection flow adjacent to a non-isothermal Wedge‖, Int. Commun. Heat Mass Tran., vol., 26, 1999, pp. 819e827. [26]. Hsiao, K., ―MHD mixed convection for viscoelastic fluid past a porous Wedge‖, Int. J. Non Lin. Mech., vol., 46, 2011, pp. 1e8.

Hedayati, F., Malvandi, A., Ganji, D. D., ―Second-law analysis of fluid flow over an isothermal moving wedge‖, Alexandria Eng. J, vol., 53, 2014, pp. 1e9. [28]. Vajravelu, K., Mukhopadhyay, S., ―Fluid Flow, Heat and Mass Transfer at Bodies of Different Shapes: Numerical Solutions‖, Academic Press, 2015. [29]. Pandey, A. K., Kumar,M., ―Effect of viscous dissipation and suction/injection on MHD nanofluid flow over a wedge with porous medium and slip‖, Alexandria Eng. J., vol. 55, No. (4), 2016, pp. 3115e3123.

Pandey, A. K., Kumar, M.,―Chemical reaction and thermal radiation effects on boundary layer flow of nanofluid over a wedge with viscous and Ohmic dissipation‖, St. Petersburg Polytech. Univ. J. Phys. Math., Vol. 3 (4), 2017, pp. 322e332.

Tufail, M. N., Butt, A. S., and Ali, A., ―Heat, source/sink effects on non Newtonian MHD fluid flow and heat transfer over a permeable stretching surface: Lie group analysis,‖ Indian J. Phys., vol. 88, 2013, pp. 75–82 https://doi.org/10.1007/s12648-013-0376-3.

Ramesh, G. K., Chamkha, A. J., and Gireesha, B.J., ―Magnetohydrodynamic flow of a non-Newtonian nanofluid over an impermeable surface with heat generation/ absorption,‖ J. Nanofluids, vol. **3**, 2014, pp. 78–84. https://doi.org/10.1166/jon.2014.1082.

Pal, D. ―Combined effects of non-uniform heat source/sink and thermal radiation on heat transfer over an unsteady stretching permeable surface‖. Commun. Nonlinear Sci. Numer. Simulat, vol. 16, 2011, pp. 1890–1904. [34]. Kumar, K. A., Reddy, J. V. R., Sugunamma, V., Sandeep, N. ―Impact of frictional heating on MHD radiative ferrofluid past a convective shrinking surface. Def. Diff. Forum, vol. 378, 2017, pp. 157–174.

Mabood, F., Ibrahim, S. M., Rashidi, M. M., Shadloo, M. S. & Lorenzini, G. ―Non – uniform heat source/sink and Soret effects on MHD non -Darcian Convective flow past a stretching sheet in a micropolar fluid with radiation‖. Int. J. Heat Mass Transf., vol. 93, 2016, pp. 674–682.

Makinde, O. D., Mabood, F. & Ibrahim, M. S. ―Chemically reacting on MHD boundary-layer flow of nanofluids over a non-linear stretching sheet with heat source/sink and thermal radiation‖. Therm. Sci., vol. 22, 2018, pp. 495–506. [37] Mabood, F., Ibrahim, S. M. & Khan, W. A. ―Effect of melting and heat generation/ absorption on Sisko nanofluid over a stretching surface with nonlinear radiation‖. Phys. Scrip., vol. 94, 2019, Artile ID: 065701.

Umavathi, J.C., and Jaweriya Sultana. ―Mixed convection of a micropolar fluid in a vertical channel with boundary conditions of third kind. International Journal of Engineering, Science and Technology‖. Vol. 3, No. 4, 2011, pp. 213-224.

Upreti, H., Pandey, A. K., Kumar, M. ―MHD flow of Ag-water nanofluid over a flat porous plate with viscous-Ohmic dissipation, suction/injection and heat generation/ absorption‖. Alexandria Eng. J., vol. 57(3), 2018, pp.1839–1847 [40]. Mabood, F., Ibrahim, S.M., Rashidi, M.M., Shadloo, M.S., Lorenzini, G. ―Non- uniform heat source/sink and Soret effects on MHD non-Darcian convective flow past a stretching sheet in a micropolar fluid with radiation‖. Int. J. Heat

Mass Transf., vol. 93, 2016, pp. 674–682.

Singh, K.,Kumar, M. ―Melting and heat absorption effects in boundary layer stagnation-point flowtowards a stretching sheet in a micropolar fluid‖. Ain Shams Eng. J., vol. 9, pp. 861–868.

Kumar, K. A., Reddy, J. R., Sugunamma, V., Sandeep, N. Magnetohydrodynamic Cattaneo–Christov flow past a cone and a wedge with variable heat source/sink‖. Alexandria Eng. J., vol. **57**(1), 2018, pp. 435–443. [43]. Kumar, K. A., Sugunamma, V., Sandeep, N., Mustafa, M.T. ―Simultaneous solutions for first order and second order slips on micropolar fluid flow across

a convective surface in the presence of Lorentz force and variable heat source/sink‖. Sci. Rep. Vol. 9(1), 2019, pp. 1–14.

Shamshuddin, M.D., Thumma, T.―Numerical study of a dissipative micropolar fluid flow past an inclined porous plate with heat source/sink‖. Propul. Pow. Res., Vol. 8(1), 2019, pp. 56–68.

Shamshuddin,M.D., Thirupathi,T., SatyaNarayana, P.V.―Micropolar fluid flow induced due to a stretching sheet with heat source/sink and surface heat flux boundary condition effects‖. J. Appl. Comput. Mech., Vol. 5(5), 2019, pp. 816–826

Waqas, H., Khan, S. U., Shehzad, S. A., Muhammad Imran. ―Significance of the nonlinear radiative flow of micropolar nanoparticles over porous surface with a gyrotactic microorganism, activation energy, and Nield's condition‖. Heat Transfer—Asian Res. Wiley, 2019, pp. 1-27.

Kuznetsov, A. V., ―The onset of nanofluid bioconvection in a suspension containing both nanoparticles and gyrotactic microorganisms‖. Int Commun Heat Mass Transf., vol. 37, 2010, pp. 1421-1425.

Kuznetsov, A. V., ―Nanofluid bioconvection in water - based suspensions containing nanoparticles and oxytactic microorganisms: oscillatory instability. Nanoscale Res Lett., vol. 6 (100), 2011, pp. 1-13.

Taseer Muhammad, Alamri, S. Z., Waqas, H., Habib, D., Ellahi, R., ―Bioconvection flow of magnetized Carreau nanofluid under the influence of slip over a wedge with motile microorganisms‖. Journal of Thermal Analysis and Calorimetry, vol. 143, 2021, pp. 945–957.

Habib, U., Abdal, S., Siddique, I., Ali, R.―A comparative study on micropolar,

Williamson, Maxwell nanofluids flow due to a stretching surface in the presence of bioconvection, double diffusion and activation energy‖. Int. Communications in Heat and Mass Transfer, vol. 127, 2021, ID. 105551. [51].

Song, YQ, Waqas, H., Khan, S.A., Khan, S.U., M. Ijaz Khan, M. I., Yu-Ming Chu, Qayyum, S. ―Nonlinear thermally radiative heat transport for brinkman type Micropolar nano – material over an inclined surface with motile microorganisms and exponential heat source‖. International Communications in Heat and MassTransfer, vol. 126, 2021, Article ID. 105351.

Khan, S. U., Bhatti, M. M., Riaz, A. ―A revised viscoelastic micropolar Nanofluid model with motile micro - organisms and variable thermal Conductivity‖. Heat Transfer. Wiley 2020; pp.1–16. DOI:10.1002/htj.21797. [53]. Abdelmalek, Z., Khan, S. U., Awais, M., Mustfa, M. S., Tlili, I. Analysis of generalized Micropolar nanofluid with swimming of microorganisms over an accelerated surface with activation energy‖. Journal of Thermal Analysis and Calorimetry, vol. 144, 2021, pp. 1051–1063.

Waqas, H., Kafait, A., Alghamdi, M., Taseer Muhammad, Alshomrani, A. S. ―Thermo – bioconvectional transport of magneto - Casson nanofluid over a wedge containing motile microorganisms and variable thermal conductivity‖.Alexandria Engineering Journal, vol. 61, 2022, pp. 2444–2454.

Uddin, Z., Manoj Kumar, Harmand, S., ―Influence of thermal radiation and heat generation/absorption on MHD heat transfer flow of a Micropolar fluid past a wedge with hall and ion slip currents. Thermal Science, Vol. 18, Suppl. 2, 2014, pp. S489-S502.

Bég, O. A., Bhargava, R., Rashidi M. M., Numerical Simulation in Micropolar Fluid Dynamics, Lambert Academic, Saarbrucken, Germany, (2011).

Gupta, D., Kumar, L., Bég, O. A., Singh, B., ― Finite element analysis of transient heat and mass transfer in microstructural boundary layer flow from porous stretching sheet‖, Comp. Thermal Sci., Vol. **6** (2), 2014, 155. doi: https://doi:https://doi.org/10.1615/ComputThermal-Scien.2014008401. Nath, G., "Similar solutions for the incompressible laminar boundary layer with pressure gradient in Micropolar fluids, Rheol. Acta **14,** 1975, 850. doi: https: // doi.org /10.1007/BF01521414.

Shaukatullah, H., Gaynes, M.A.,―Comparative evaluation of various types of heat sinks for thermal enhancement of surface mount plastic packages‖, Int. J. Micro. Electron. Packag. Vol. **18,** (1995) 252.

Cheng, W. T., Huang, C. N., ―Unsteady flow and heat transfer on an accelerating surface with blowing or suction in the absence and presence of a heat source or sink‖, Chem. Eng. Science, vol. 59, (2004), 771.

Winter, H. H., ―Viscous dissipation in shear flows of molten polymers‖, Adv. Heat Transf., vol.**13 (**3), 1977, pp. 205- 264 doi:https://doi.org/10.

1016 /S0065-2717(08)70224-7.

Yih, K. A., ―MHD Forced Convection Flow adjacent to a Non-Isothermal Wedge, *Int Comm. Heat Mass Transfer, 26* (1999), 6, pp. 819-827.

[Chamka, A. J., Mujtaba, M., Quadri, A., Camille Issa. ―Thermal Radiation Effects on MHD Forced Convection Flow adjacent to a Non-Isothermal Wedge in the Presence of Heat Source or Sink‖, Heat Mass Transfer, vol. 39 (4), 2003, pp. 305-312.

Ishak, A., Nazar, R., Pop, I., ―MHD Boundary-Layer Flow of a Micropolar Fluid past a Wedge with Constant Wall Heat Flux, Communications Nonlinear Science Numerical Simulation‖, vol. 14 (1), 2009, pp. 109-118.